# THREE-DIMENSIONAL REGIONAL DYNAMICS OF THE NORMAL MITRAL ANULUS DURING LEFT VENTRICULAR EJECTION

Julie R. Glasson, MD[a]
Masashi Komeda, MD, PhD[a]
George T. Daughters, MS[a, b]
Marek A. Niczyporuk, BS[a]
Ann F. Bolger, MD[c, d]
Neil B. Ingels, PhD[a, b]
D. Craig Miller, MD[a, e]

**The mitral anulus is a dynamic structure that undergoes alterations in size and shape throughout the cardiac cycle, contracting during systole. Numerous reports have shown this systolic orifice reduction to be due chiefly to posterior annular contraction, whereas the anterior perimeter was unchanged. Segmental motion of the mitral anulus from true in vivo three-dimensional data, however, has not been described. We used radiopaque markers and simultaneous biplane videofluoroscopy to measure the lengths of mitral anular segments in seven closed-chest, sedated dogs. Eight markers were placed equidistant from each other around the mitral anulus. As viewed from the left atrium, segment 1 began at the posteromedial commissure, and the remaining segments were numbered sequentially clockwise around the anulus (that is, the posterior mitral anulus encompassed segments 1 to 4 and the anterior anulus encompassed segments 5 to 8). Marker image coordinates obtained from two orthogonal views 7 to 12 days after implantation were merged to construct three-dimensional marker coordinates at end-diastole and end-systole. From end-diastole to end-systole, mean annular area decreased by 11% ± 8% (5.5 ± 0.9 $cm^2$ to 4.9 ± 0.8 $cm^2$, $p = 0.005$) and perimeter by 5% ± 4% (8.8 ± 0.7 cm to 8.3 ± 0.7 cm, $p < 0.01$). Mitral annular segmental percent systolic shortening (negative values indicate lengthening) were as follows (mean ± standard deviation): segment 1, 7% ± 9%; segment 2, 8% ± 10%; segment 3, 16% ± 6%; segment 4, 10% ± 7%; segment 5, −4% ± 5%; segment 6, −7% ± 7%; segment 7, 3% ± 2%; and segment 8, 6% ± 5%. With the exception of segment 1, all posterior (2 to 4) and two anterior (7 and 8) mitral annular segments contracted significantly ($p \leq 0.05$ vs zero, paired $t$ test). Two anterior annular segments (5 and 6, regions overlapping aortic-mitral continuity), however, unexpectedly *lengthened* during left ventricular systole. We conclude that the anterior mitral anulus may be a much more dynamic component of the mitral apparatus that previously thought. Such heterogeneous dynamic annular motion should be taken into account when various mitral valve reparative techniques are being designed. (J THORAC CARDIOVASC SURG 1996;111:574-85)**

From the Department of Cardiovascular and Thoracic Surgery[a] and the Division of Cardiovascular Medicine,[c] Stanford University School of Medicine, Stanford, Calif., the Cardiac Surgery[e] and Cardiology Sections,[d] Department of Veterans Affairs Medical Center, Palo Alto, Calif., and the Department of Cardiovascular Physiology and Biophysics,[b] Research Institute of the Palo Alto Medical Foundation, Palo Alto, Calif.

Supported by grant HL-29589 from the National Heart, Lung, and Blood Institute, and the Veterans Administration Medical Research Service. Drs. Glasson and Komeda are Carl and Leah McConnell Cardiovascular Surgical Research Fellows. Dr. Glasson was also supported by The Thoracic Surgery Foundation Research Fellowship Award.

Read at the Twenty-first Annual Meeting of The Western Thoracic Surgical Association, Coeur d'Alene, Idaho, June 21-24, 1995.

Address for reprints: D. Craig Miller, MD, Department of Cardiovascular and Thoracic Surgery, Falk Cardiovascular Research Center, Stanford University School of Medicine, Stanford, CA 94305-5247.

**12/6/70797**

The mitral anulus is a dynamic structure that undergoes alterations in size and shape throughout the cardiac cycle, contracting during systole. Early experiments demonstrated a reduction in the size of the mitral orifice during left ventricular (LV) ejection in isolated hearts[1] and in perfused hearts in open-chest animals.[2] These experiments, however, could not discern motion of the anterior mitral anulus from that of the posterior anulus. Tsakiris and associates[3] performed the first studies assessing regional mitral annular motion in the early 1970s. This group sutured perforated lead beads to the mitral anulus in dogs and followed mitral annular motion cinefluoroscopically. They noted that systolic mitral annular contraction was due principally to posterior annular contraction, with the anterior anulus remaining unchanged in size throughout the cardiac cycle; however, they could not reconstruct true three-dimensional (3-D) coordinates for each marker site on the anulus. More recent studies of mitral annular motion with echocardiography[4, 5] also described systolic orifice narrowing but could not investigate 3-D regional mitral annular dynamics. All previous studies, however, were limited by the inability to track discrete sites on the mitral apparatus in 3-D space with respect to a fixed external laboratory coordinate system.

We hypothesized that systolic 3-D mitral annular motion was homogeneous. In this study we used myocardial marker technology[6] to investigate precise in vivo 3-D motion of the normal canine mitral anulus. By suturing eight markers circumferentially around the anulus, and then studying the motion of these markers with simultaneous biplane videofluoroscopy at an imaging rate of 60 Hz with simultaneous digitization and recording of the electrocardiogram (ECG) and LV pressure, we were able to analyze 3-D regional changes in size and shape of the mitral anulus throughout the cardiac cycle.

## Materials and methods

**Surgical preparation.** Seven healthy adult mongrel dogs (30 ± 5 kg) of either sex were premedicated with acepromazine (0.01 to 0.05 mg/kg intramuscularly) and atropine sulfate (0.05 mg/kg intravenously [IV]), anesthetized with sodium thiopental (25 mg/kg intravenously), intubated, and placed on artificial ventilation (Ohio Anesthesia Ventilator, Madison, Wis.). General anesthesia was maintained with 1% to 2.2% inhalational isoflurane and supplemental oxygen. An arterial catheter was placed percutaneously into the left femoral artery and connected to a micromanometer-tipped pressure transducer (MPC-500, Millar Instruments, Inc., Houston, Tex.), previously zeroed in a 37° C water bath to monitor systemic arterial pressure. A left thoracotomy was performed through the fifth intercostal space, and superior and inferior vena caval pneumatic occluders (In Vivo Metric Systems, Healdsburg, Calif.) were placed to allow transient alterations in preload. The heart was suspended in a pericardial cradle, and miniature tantalum radiopaque helices (inner diameter 0.8 mm, outer diameter 1.3 mm, length 1.5 to 3.0 mm [some with variable small extensions or "tails" to facilitate subsequent radiographic identification]) were inserted into the LV wall and septum. Markers were placed on the obturator of a modified spinal needle (20 gauge), inserted through a stab wound in the epicardial surface, and deposited into the subepicardium by withdrawal of the obturator from the sheath. As depicted in Fig. 1, eight markers were placed into the LV subepicardium along four equally spaced longitudinal meridians around the LV, including anterior (from the origin of the left anterior descending coronary artery to the apex), lateral (obtuse margin), posterior (inferior wall along the posterior descending coronary artery), and septal walls. Each meridian contained markers at two levels, in the basal-equatorial and apical-equatorial planes. A ninth marker was placed at the LV apex. The septal markers were inserted with 2-D echocardiographic guidance to place the markers at the desired sites on the right ventricular septal endocardial surface. This arrangement permitted 3-D visualization of the LV silhouette in both 45-degree right anterior oblique and 45-degree left anterior oblique videofluoroscopic images.

After LV subepicardial marker placement was completed, the animal was heparinized (300 IU/kg IV) and cardiopulmonary bypass using a roller pump (Pemco, Cleveland, Ohio) with a bubble oxygenator (Harvey H-1300, Bard Cardiopulmonary, Santa Ana, Calif.) was instituted; a 14F or 16F arterial cannula was inserted into the right femoral artery, and a two-stage venous cannula was inserted into the right atrium and inferior vena cava. The ascending aorta was crossclamped, and the heart was arrested with cold cardioplegic solution delivered into the aortic root.

The left atrial appendage was opened, exposing the mitral apparatus. As depicted in Figs. 1 and 2, eight miniature tantalum radiopaque markers were sutured at equal distances around the circumference of the mitral anulus, one near each commissure and three along the perimeters of the anterior and posterior leaflets. An implantable Koenigsberg pressure transducer (Koenigsberg Instruments, Inc., Pasadena, Calif.) was placed in the LV lumen via the apex for subsequent monitoring of LV chamber pressure. The heart was rewarmed, the aortic crossclamp released, the left atriotomy closed, and the animal weaned from CPB. Heparin was reversed with protamine, and the pericardium was loosely reapproximated. To minimize immediate postoperative pain, we placed an intercostal block (20 ml 0.25% bupivicaine) at the fourth, fifth, and sixth intercostal spaces. Chest tubes were placed, and the incision was closed. The animals were allowed to recover in the intensive care unit of the Stanford University Department of Laboratory Animal Medicine with oxymorphone hydrochloride (Numorphan 0.05 to 0.2 mg/kg IV, DuPont Merck Pharma, Manatic, Puerto Rico) to minimize incisional discomfort.

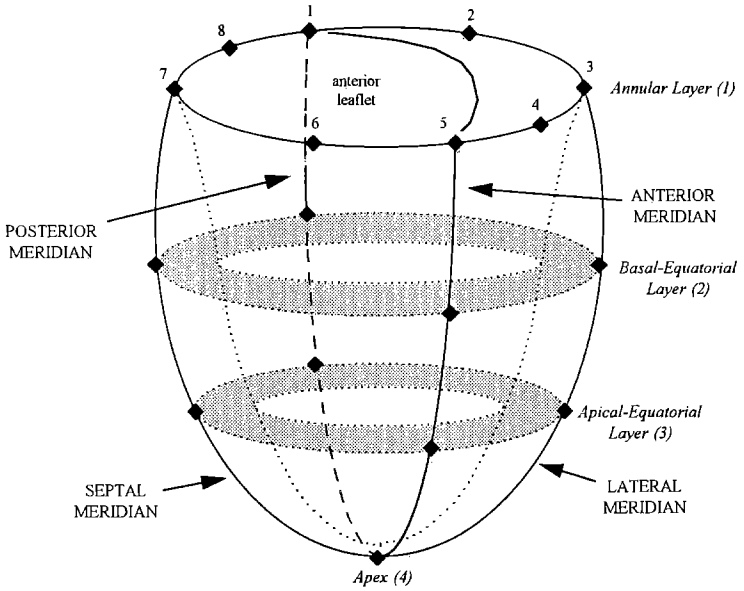


**Fig. 1.** Representation of the nine subepicardial marker array in the left ventricle. The eight mitral annular marker numbers are also shown. Layer numbers (shown in *parentheses*) were used in the LV volume calculation equations.

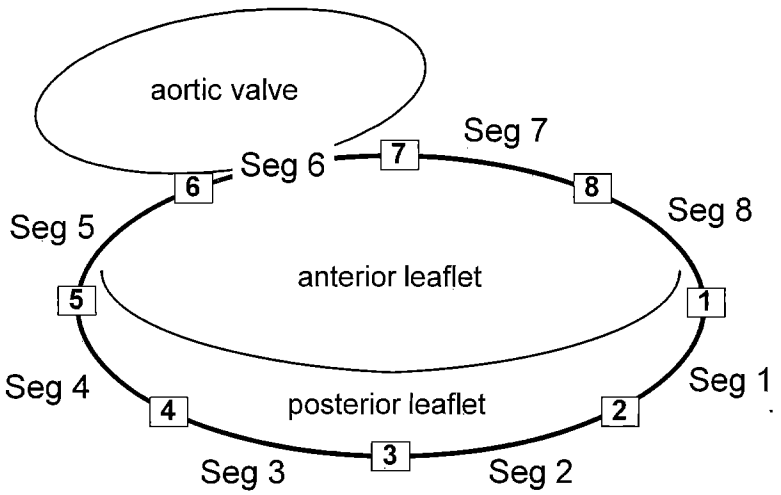


**Fig. 2.** Representation of the eight marker array on the mitral anulus, as viewed from the left atrium. Segment *(Seg)* and marker numbers *(inside small squares)* are shown. The region of aortic-mitral continuity overlaps segments 5 and 6.

**Experimental protocol.** After 7 to 12 days (9 ± 2 days [mean ± standard deviation]), the animal was taken to the cardiac catheterization laboratory for hemodynamic and videofluorographic data acquisition. Mild sedation was accomplished with diazepam (5 mg IV) and supplemental ketamine (5 mg/kg IV), administered as needed. A micromanometer-tipped catheter (Millar MPC-500) was zeroed in a 37° C water bath and advanced via a left femoral artery cutdown into the ascending aorta for aortic pressure monitoring. To minimize reflex sympathetic and parasympathetic responses that occur in conscious animals, we produced autonomic blockade with esmolol (0.25 to 0.4 mg/kg per minute IV infusion, titrated to reduce the heart rate below 120 beats/min) and atropine sulfate (0.02 to 0.04 mg/kg IV). UL-FS49 (Boehringer-Ingelheim, Ridgefield, Conn.), a highly specific negative chronotropic agent that does not change the QT interval, inotropic state, or systolic or diastolic blood pressure,[7] was administered (4 to 6 mg IV single dose) to lower heart rate further, if needed. Such heart rate reduction was neces-

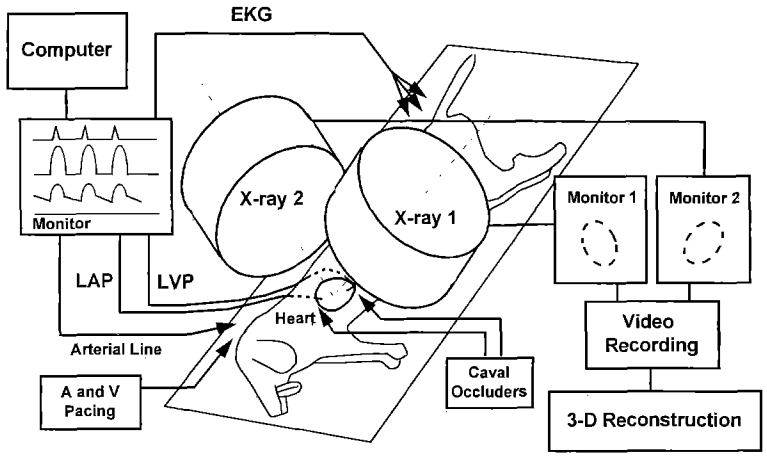


**Fig. 3.** Schematic diagram of data acquisition set-up. The two x-ray beams were set at 45-degree right anterior oblique and 45-degree left anterior oblique positions. *LAP,* Left atrial pressure; *LVP,* left ventricular pressure; *A,* atrial; *V,* ventricular; *EKG,* electrocardiogram.

sary to facilitate subsequent cinefluoroscopic visualization and tracking of marker motion. Data were obtained with dogs in normal sinus rhythm, except for dog 7, which was atrially paced at 120 beats/min because of intrinsic atrioventricular dissociation with a slower heart rate. Baseline hemodynamic and biplane videofluoroscopic data recordings were obtained during steady-state conditions and over a physiologic range of peak LV systolic pressures during vena caval occlusion. The dogs were allowed to recover for 3 to 5 minutes before further data acquisition. Any data acquisition sequences containing premature ventricular contractions were discarded and subsequently repeated.

All animals received humane care in compliance with the "Principles of Laboratory Animal Care" formulated by the National Society for Medical Research and the "Guide for Care and Use of Laboratory Animals" prepared by the National Academy of Sciences and published by the National Institutes of Health (NIH Publication No. 85-23, revised 1985). This study was approved by the Stanford Medical Center Laboratory Research Animal Review Committee and conducted according to Stanford University policy.

**Data acquisition.** All imaging studies were conducted with the animal in the right lateral decubitus position with the use of a Philips Optimus 2000 biplane Lateral ARC 2/Poly DIAGNOST C2 system (Philips Medical Systems, North America Company, Pleasanton, Calif.) with the image intensifiers in the 2-inch fluoroscopic mode (Fig. 3). The 45-degree right anterior oblique and left anterior oblique biplane images were recorded simultaneously on Sony U-Matic 5800 ¾-inch videocassette recorders with the x-ray pulses synchronized by a master sync oscillator at 60 Hz. The analog LV pressure signal was digitized and recorded in digital format on each individual video image with a custom-designed intelligent video controller (Grey Engineering Corp., Los Angeles, Calif.); the ECG R wave was detected electronically and digitally encoded on the videotape as an end-diastolic timing marker. At the completion of the study, images of grids containing 1 cm squares and biplane images of a 3-D helical phantom of known dimensions were recorded to determine radiographic distortion and magnification factors. The 2-D coordinates of each marker in each projection were digitized frame by frame with a semi-automated, computerized myocardial marker detection system (Hewlett-Packard RS/20, Palo Alto, Calif.) equipped with Matrox MVP/AT/NP image processing boards (Dorval, Quebec, Canada) and custom-designed image-processing and digitization software developed in our laboratory.[8] The data from the two views were corrected for x-ray magnification and distortion, and the right anterior oblique and left anterior oblique marker coordinates were merged with custom-designed software to yield 3-D coordinates of each marker every 16.7 msec, as previously described.[9]

During data acquisition, two channels of analog data (LV pressure and surface lead ECG) were acquired and digitized simultaneously at 240 Hz with a 486-based microcomputer (486-33, JDR Microdevices Inc., San Jose, Calif.) with a high-speed data acquisition card (DT 3831-G, Data Translation Inc., Marlboro, Mass.) controlled by commercially available software (Labtech Control 3.2.0, Laboratory Technology Corp., Wilmington, Mass.). These analog signals were simultaneously recorded on a Vidco multichannel color display recorder (model 580CDR/16, Vidco Inc., Beaverton, Ore.) at a paper speed of 25 mm/sec. The 240 Hz pressure data were merged with the 60 Hz marker-derived geometry data by aligning the LV pressure waves (or ECG R waves) from the two data sources and calculating a convolution of the 240 Hz and 60 Hz signals to be matched.

**Data analysis**

*Hemodynamics.* To minimize the effects of intrathoracic pressure variation, we chose only end-expiratory beats for analysis. The LV pressure signal was differentiated with respect to time to determine peak positive rate of rise of LV pressure ($dP/dt_{max}$) and peak negative LV dP/dt ($-dP/dt_{max}$). For each cardiac cycle, the time of

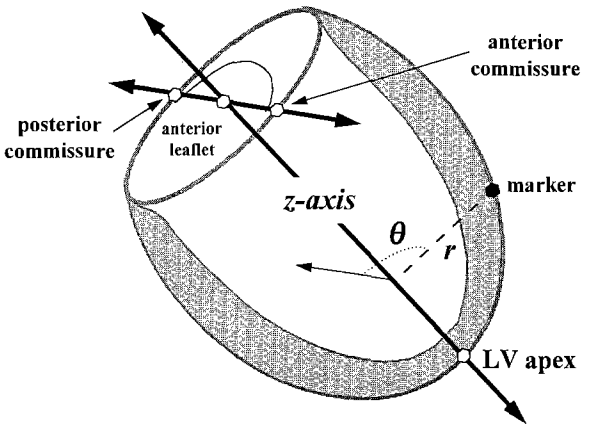


**Fig. 4.** Cylindrical coordinate system defined with its origin at the midpoint of the commissural markers with the negative *z*-axis directed toward the LV apical marker. The *z*-axis coordinate of each mitral annular marker was calculated at end-diastole and end-systole. *r,* Perpendicular distance from the *z*-axis to a marker of interest; *theta (θ),* angle in radians between the position of the posterior commissure (defined as zero radians) and *r* for any marker of interest.

end-diastole was defined as the videofluoroscopic frame containing the ECG R wave and end-systole was defined as the videofluoroscopic frame immediately before the frame that contained the point of maximum negative LV dP/dt. LV ejection fraction was calculated as ([EDV − ESV]/EDV) · 100%, where EDV and ESV are LV end-diastolic and end-systolic volumes calculated as described below.

*LV volume.* Instantaneous LV volume was calculated with a multiple cylindrical/cone model.[10] The eight epicardial markers, eight annular markers, and one apical marker (see Fig. 1) define three cross-sectional marker layers from base to apex (annular, basal-equatorial, and apical-equatorial). LV volume is represented as the sum of the volumes of two elliptical cylinders (between anulus and basal-equatorial layers and between basal-equatorial and apical-equatorial layers) and one elliptical cone (between apical-equatorial layer and apex).

*Systolic LV function.* Systolic performance was assessed as LV end-systolic elastance, measured from the end-systolic pressure-volume relationship.[11-13] We determined LV end-systolic pressure ($P_{es}$) and volume ($V_{es}$) instantaneously during abrupt preload reduction using an iterative computer algorithm to define end-systolic pressure-volume relationship.[14, 15] A line was fitted to these end-diastolic points by least-squares linear regression of the form: $P_{es} = E_{es} (V_{es} - V_0)$, where $E_{es}$ and $V_0$ are the slope and volume axis intercept, respectively.

*Mitral annular dynamics.* Mitral annular segmental lengths between adjacent markers were computed from the 3-D annular marker data at end-diastole and end-systole. Percent shortening for each segment was calculated as ([EDL − ESL]/EDL) · 100%, where EDL and ESL are end-diastolic and end-systolic lengths; negative values indicated lengthening during LV ejection. Mitral annular area and perimeter were computed from 3-D marker coordinates, without assuming circular or planar geometry. The perimeter of the mitral anulus was calculated as the sum of the 3-D lengths of the eight contiguous segments (Fig. 2). The annular area was computed as the summation of six triangular areas derived from triplets of annular marker coordinates. Percent change for area and perimeter were calculated as ([EDA − ESA]/EDA) · 100% and ([EDC − ESC]/EDC) · 100%, where EDA and ESA are end-diastolic and end-systolic area and EDC and ESC are end-diastolic and end-systolic perimeter. A cylindrical coordinate system, depicted in Fig. 4, was defined with its origin at the midpoint of the commissural markers (markers 1 and 5), with the negative *z*-axis directed toward the LV apical marker. The *z*-axis coordinate of each mitral anulus marker was calculated at end-diastole and end-systole. By means of this convention, positive *z* coordinates were closer to the left atrium and negative *z* coordinates were located closer to the LV apex.

**Statistical analysis.** All data are reported as mean plus or minus one standard deviation. Mitral anulus area, perimeter, segmental length measurements, and marker *z* coordinates at end-diastole and end-systole were compared by Student's *t* test for paired observations. Evaluation of segmental percent shortening was performed by two-way analysis of variance with segment number as an independent variable and dog identity entered as a dummy variable to control for interanimal differences; when indicated by a significant *F* statistic ($p \leq 0.05$), segmental differences were examined by means of the Bonferroni correction for multiple comparisons.

## Results

Postmortem examination of the excised hearts revealed all LV markers to be within 1 mm of the epicardial surface. All eight annular markers were within 1 mm of the mitral anulus, as defined by the mitral leaflet–left atrium junction.

**Hemodynamics.** Mean heart rate for all dogs was 106 ± 10 beats/min and average ejection fraction was 22% ± 5%, $E_{es}$ 2.1 ± 0.5 mm Hg/ml, and $dP/dt_{max}$ 1614 ± 182 mm Hg/sec. As expected, autonomic blockade with esmolol resulted in diminished end-systolic chamber elastance.

**Mitral annular dynamics.** Table I summarizes mitral annular area, perimeter, and segment lengths at end-diastole and end-systole (refer to Fig. 2 for marker and segment number key). Mitral annular area and perimeter decreased from end-diastole to end-systole in all dogs. Fig. 5 shows typical changes in mitral annular area, mitral annular perimeter, and LV pressure versus time for three consecutive beats in one representative dog. As can be seen, significant reduction in area and perimeter occurred from end-diastole to end-systole.

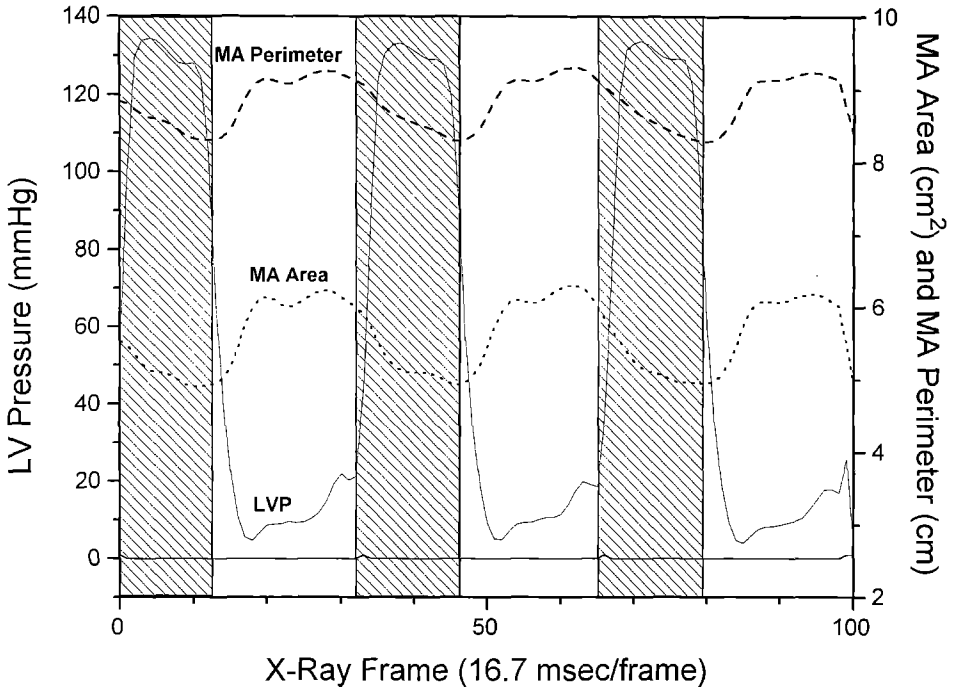


**Fig. 5.** Representative baseline data from three cardiac cycles from one dog, demonstrating the changes in annular area, annular perimeter, and LV pressure versus x-ray frame number (1 frame = 16.7 msec). The *shaded areas* are between the ECG R-wave marker (end-diastole) and maximum negative dP/dt minus 1 frame (end-systole), which defined LV ejection in this experiment. *MA,* Mitral anulus; *LVP,* LV pressure.

**Table I.** *Mitral annular measurements*

| *Variable* | *End-diastole* | *End-systole* | *SS (%)* | *p Value* |
|---|---|---|---|---|
| Area ($cm^2$) | 5.5 ± 0.9 | 4.9 ± 0.8 | 11.4 ± 7.7 | 0.005 |
| Perimeter (cm) | 8.8 ± 0.7 | 8.3 ± 0.7 | 5.2 ± 3.9 | <0.01 |
| Segment 1 (mm) | 9.1 ± 2.2 | 8.5 ± 2.2 | 6.5 ± 8.9 | NS |
| Segment 2 (mm) | 11.0 ± 2.3 | 10.1 ± 2.4 | 8.4 ± 9.8 | 0.05 |
| Segment 3 (mm) | 15.2 ± 1.2 | 12.8 ± 1.2 | 15.9 ± 6.2 | <0.001 |
| Segment 4 (mm) | 9.0 ± 2.8 | 8.1 ± 2.5 | 9.6 ± 7.3 | 0.02 |
| Segment 5 (mm) | 10.2 ± 2.1 | 10.7 ± 2.3 | −4.1 ± 4.8 | 0.05 |
| Segment 6 (mm) | 11.6 ± 2.5 | 12.3 ± 2.2 | −7.3 ± 6.6 | <0.01 |
| Segment 7 (mm) | 10.5 ± 2.6 | 10.2 ± 2.5 | 3.0 ± 2.3 | 0.01 |
| Segment 8 (mm) | 11.0 ± 0.9 | 10.4 ± 1.1 | 5.7 ± 4.9 | 0.02 |

Data are expressed as mean ± 1 standard deviation; $n = 7$ dogs. *SS,* Systolic shortening as a percentage (negative values indicate lengthening); $p$ value of systolic percent shortening versus zero by Student's $t$ test for paired observations; $p \leq 0.05$ is significant.

Five of the eight mitral annular segments shortened significantly during LV ejection (Table I). Segment 1, on the posterior anulus adjacent to the posterior commissure, did not change in length significantly from end-diastole to end-systole. Unexpectedly, two segments (5 and 6) in the anterior anulus *lengthened* during LV ejection. This region overlaps the area of aortic-mitral continuity, with marker number 6 close to the left fibrous trigone. Fig. 6 shows mean percent systolic shortening for each segment graphically. Statistical analysis with two-way analysis of variance demonstrated that segment number was an important determinant of length change ($p < 0.0001$). The greatest shortening was found in segment 3 (15.9% ± 6.2%, $p < 0.001$ vs zero), which is roughly in the middle of the posterior anulus. Segment 6, nearest the area of aortic-mitral continuity, showed the greatest lengthening from end-diastole to end-systole (−7.3% ± 6.6%, $p < 0.01$ vs zero). The changes between these two segments were statistically different by post-hoc $t$ test (percent change segment 3 vs percent change segment 6, $p = 0.0001$).

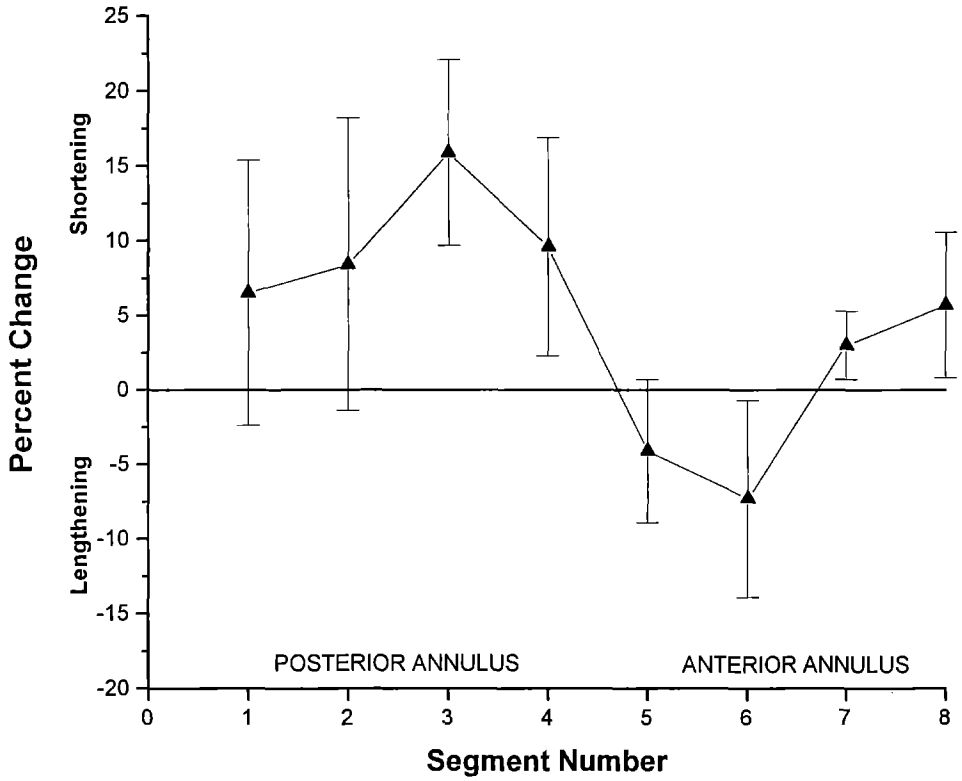


**Fig. 6.** Percent systolic shortening for all eight mitral annular segments (from end-diastole to end-systole). Data are mean percent shortening for each segment (negative values indicate lengthening). *Error bars* represent ± standard deviation.

In addition to segmental length changes, we compared the $z$ coordinates of each mitral anulus marker at end-diastole and end-systole to assess change in mitral annular shape. Fig. 7 graphically demonstrates mitral anulus marker positions along the $z$-axis. As can be seen from this graph, at end-diastole the anterior mitral anulus has positive $z$ coordinates and the posterior anulus has negative $z$ coordinates, but at end-systole the $z$ coordinates of the posterior anulus decrease ($p < 0.005$ for marker 3) and the $z$ coordinates of the anterior anulus increase ($p < 0.001$ for markers 6 and 7), resulting in a shape increasingly concave toward the left atrium. Although markers 3, 6, and 7 all move upward toward the left atrium at end-systole relative to end-diastole, marker 3 on the posterior anulus remains below the plane of the intercommissural reference point, resulting in a "tilted saddle/ski jump" shape of the mitral anulus.

## Discussion

In this study, myocardial marker technology was used to investigate the in vivo 3-D regional motion of the mitral anulus in the closed-chest, sedated dog. In addition to the expected shrinkage of annular area and perimeter during systole, we found the mitral anulus to have an inhomogeneous pattern of systolic contraction: whereas the posterior anulus shortened, two segments of the anterior anulus lengthened significantly.

**Hemodynamics.** All animals studies were healthy adult mongrel dogs. Except in dog 7 (atrially paced throughout data collection), all data were obtained in normal sinus rhythm during autonomic blockade with esmolol and atropine sulfate. Inasmuch as the hemodynamic parameters for dog 7 were not statistically different from those of the other animals, the mitral annular measurements presented are for all seven study animals. As noted earlier, average slope for the study group is low, showing mildly depressed LV function, which is likely due to the β-adrenergic blockade.

**Mitral annular dynamics.** Mitral annular area and perimeter decreased from end-diastole to end-systole in all dogs, although our measurements of systolic annular area change are somewhat lower

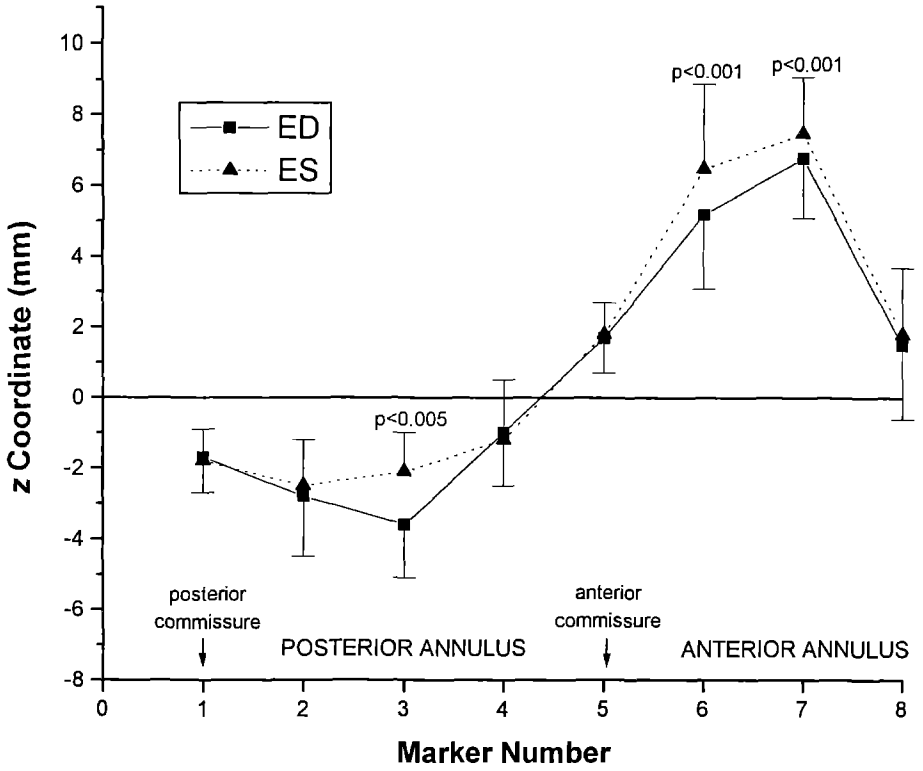


**Fig. 7.** Mitral annular marker position (*z* coordinates) at end-diastole and end-systole. See Fig. 4 for orientation. Data are mean marker position (mm) with error bars representing 1 standard deviation. Note that marker numbers 3, 6, and 7 ascended significantly ($p < 0.005$) toward the left atrium during systole with respect to their end-diastolic positions. *ED,* End-diastole; *ES,* end-systole.

than 19% to 34% previously reported in the literature.[3-5, 18] Several factors could explain this disparity. First, although our data (Fig. 5) support the presence of presystolic narrowing of the anulus (as described first by Tsakiris and associates[3]), the area and perimeter calculations in our study incorporated *only the period of LV ejection* and therefore do not reflect this presystolic narrowing. Second, our calculations were made from distinct, reproducible time points in the cardiac cycle, that is, ECG R wave for end-diastole and maximum negative dP/dt for end-systole, as opposed to maximum and minimum anulus size, which may vary in timing from beat to beat and from animal to animal. Third, the animals in this study were autonomically blocked and had mildly depressed LV function, which likely diminished the overall shortening of the mitral annular segments along with overall LV contractility.

This study is the first to describe in vivo beat to beat segmental mitral annular dynamics computed from 3-D geometric data. Previous studies have only described annular dynamics in 2-D[1-5] and therefore did not show the 3-D length changes in the anterior anulus that we observed. Our data support the traditionally accepted notion of posterior annular contraction during LV systole.[1-3] We found the midposterior region of the mitral anulus to shorten the greatest amount during systole. Conversely, we unexpectedly observed systolic *lengthening* in the anterior regions of the mitral anulus. In this study, mitral annular segments 5 and 6 lengthened significantly from end-diastole to end-systole; these segments overlap the area of aortic-mitral continuity. This region has traditionally been accepted as fibrous and rigid, fixed by the fibrous trigones.[19] The area of segmental lengthening was also noted to have greater positive *z* coordinates at end-systole (see Fig. 7), a finding consistent with more left atrially directed displacement of the anterior mitral anulus, as recently reported with magnetic resonance imaging techniques used to analyze the motion of the mitral anulus.[18] This upward curvature of the anterior mitral anulus toward the aortic valve results in an annular shape somewhat like a ski

jump. Cineradiography of patients with *flexible* annuloplasty rings in situ showed a similar configuration.[19]

Lengthening of the anterior mitral anulus during systole may be due to several influences. Because the remainder of the mitral anulus contains muscular fibers,[20] it is possible that this region of passive fibrous tissue is elongated during systole by the active contraction of the other surrounding parts of the anulus. Additionally, lengthening of the anterior mitral anulus during systole could be related to dynamic systolic expansion of the aortic root.[21, 22] This is an unlikely explanation, however, because aortic root expansion occurs chiefly during *early* systole, whereas lengthening of segments 5 and 6 occurred *throughout* LV ejection and peaked in *late* systole. Anatomic studies of gross morphology and fiber geometry in the heart have revealed an inhomogeneous pattern of myocardial fibers in the mitral ring.[23-25] Dissection of the basal regions of the heart has displayed superficial myocardial fibers running from the external to the internal surface of the LV and inserting into the collagenous ring of the mitral valve.[23] Such insertions could possibly explain lengthening in this area of the mitral anulus during LV contraction; these fibers shorten with LV contraction and therefore may pull the attached part of the mitral ring as they shorten. Further 3-D studies of mitral annular motion and adjacent LV basal motion are needed to elucidate fully the mechanism(s) responsible for lengthening of the anterior mitral anulus.

**Clinical implications.** These findings demonstrate that the mitral anulus is a more dynamic structure than previously thought, with some regions lengthening while the overall perimeter shortens during LV ejection. Such heterogeneous motion of the anulus is probably important for normal mitral valvular function and may be closely linked to overall LV systolic function. The upward displacement of the anterior mitral anulus away from the LV apex at end-systole (relative to end-diastole) may possibly minimize resistance to LV outflow during ejection. In fact, van Rijk-Zwikker and associates[26] found that rigid fixation of the mitral anulus with either a ring or a prosthetic valve restricted the movement of the basal LV wall and impeded LV systolic pressure development. They also found that flexible rings interfered less with the normal movement of the mitral anulus than did rigid rings and that a stiff anulus was pushed underneath the aortic valve during systole. This abolished the upward displacement of the anterior mitral anulus (as observed in this experiment) and caused narrowing of the LV outflow tract, with resulting mild outflow tract obstruction.[27] This mechanism has been alluded to as a cause of clinical LV outflow tract obstruction in two patients after mitral valvuloplasty with a Carpentier-Edwards ring (Baxter Healthcare Corp., Edwards Div., Santa Ana, Calif.).[28] Although several studies indicate that rigid fixation of the mitral anulus does not impair LV systolic function,[16, 17] those studies were either acute, open-chest preparations or they were subacute studies (1 to 6 weeks after the operation) that did not directly investigate LV outflow tract obstruction and the long-term effects of rigid annular fixation. Additionally, these studies were performed on healthy dogs, and it is likely that maintenance of normal mitral annular motion is more important in diseased hearts with volume overload and chronic mitral regurgitation than in normal hearts. Indeed, a recent study by David and colleagues[29] indicated that patients with a flexible annuloplasty ring have better LV systolic function than patients with a rigid annuloplasty ring early after mitral valve reconstruction for chronic regurgitation.

One major clinical implication of these findings pertains to the sizing of annuloplasty rings, which fix the mitral anulus as its *end-systolic* size. Because the anterior mitral anulus does not appear to maintain constant size and shape during systole, as previously thought, perhaps the intertrigonal and intercommissural distances do not give an accurate estimation of the proper ring size to use. Perhaps the area of the anterior mitral leaflet yields a better approximation of appropriate annuloplasty ring size, but this remains to be demonstrated clearly.

**Limitations.** Inherent limitations of using myocardial markers include 3-D spatial accuracy and time resolution. With this system, determination of marker position is accurate and reproducible, with a mean overall error of $0.1 \pm 0.6$ mm.[9] Changes in marker positions every 16.7 msec were detected with this system, but the position of markers between these sampling points could not be determined.

Perhaps the major limitation of this study is the fact that the animals had normal hearts and were autonomically blocked to reduce heart rate and the influence of reflex sympathetic and parasympathetic responses that occur in conscious animals. Because of the autonomic blockade, the hearts studied had mildly depressed LV function and therefore likely had depressed systolic mitral annular motion as

well. Consequently, these data may not reflect annular motion that occurs in nonautonomically blocked animals and human subjects. The annular dynamics observed, however, might be even more pronounced under normal and hypercontractile conditions.

The possibility of mitral markers interfering with normal annular motion is minimal because the markers are very small, weighing less than 30 mg each. Additionally, 2-D echocardiography revealed no obvious differences in annular motion before and after marker placement.

Finally, this study was conducted in dogs, which have a greater muscular component of the cardiac endoskeleton than do human beings.[3] Consequently, these findings may not be totally applicable to human beings, and particularly to human hearts with chronic mitral regurgitation and volume overload. In the case of chronic regurgitation, mitral annular dynamics are likely to be quite different. Further 3-D studies in other animal models, with and without chronic mitral regurgitation, are necessary before optimizing surgical procedures for human beings. Such a study using an ovine model is currently in progress in this laboratory to investigate whether our present findings are specific to the dog.

We gratefully acknowledge the help of Byron W. Brown, PhD, Professor of Biostatistics at Stanford University, and the expert technical assistance of Mary K. Zasio, BA, Erin K. Schultz, BS, Cynthia E. Handen, BA, Geraldine C. Derby, RN, BS, Diana Levitt, BA, Albert Chang, BS, and Carol W. Mead, BA, in the performance of this work and Phoebe Taboada for her help in preparing the manuscript and figures.

REFERENCES

1. Smith HL, Essex HE, Baldes RJ. A study of the movements of heart valves and of heart sounds. Ann Intern Med 1950;33:1357-9.
2. Padula RT, Cowan GSM Jr, Camishion RC. Photographic analysis of the active and passive components of cardiac valvular action. J THORAC CARDIOVASC SURG 1968;56:790-8.
3. Tsakiris AG, von Bernuth G, Rastelli GC, Bourgeois MJ, Titus JL, Wood EH. Size and motion of the mitral valve annulus in anesthesized intact dogs. J Appl Physiol 1971;30: 611-8.
4. Ormiston JA, Shah PM, Tei C, Wong M. Size and motion of the mitral valve annulus in man. I. A two-dimensional echocardiographic method and findings in normal subjects. Circulation 1981;64:113-20.
5. Toumandis ST, Sideris DA, Papmichael CM, Moulopoulos SD. The role of mitral annulus motion in left ventricular function. Acta Cardiol 1992;47:331-48.
6. Ingels NB, Daughters GT, Stinson EB, Alderman EL. Measurement of midwall myocardial dynamics in intact may by radiography of surgically implanted markers. Circulation 1975;52:859-67.
7. Schipke JD, Harasawa Y, Sugiura S, Alexander J, Burkhoff D. Effect of a bradycardic agent on the isolated blood-perfused canine heart. Cardiovasc Drugs Ther 1991;5:481-8.
8. Niczyporuk MA, Miller DC. Automatic tracking and digitization of multiple radiopaque myocardial markers. Comput Biomed Res 1991;24:129-42.
9. Daughters GT, Sanders WJ, Miller DC, Schwarzkopf A, Mead CW, Ingels NB. A comparison of two analytical systems for three-dimensional reconstruction from biplane videoradiograms. Proc Comp Cardiol (IEEE) 1988;15:79-82.
10. Yun KL, Rayhill SC, Niczyporuk MA, et al. Mitral valve replacement in dilated canine hearts with chronic mitral regurgitation: importance of the mitral subvalvular apparatus. Circulation 1991;84(Suppl):III112-24.
11. Sagawa K. The end-systolic pressure-volume relation of the ventricle: definition, modifications and clinical use. Circulation 1981;63:1223-7.
12. Kass DA, Maughan WL. From $E_{max}$ to pressure-volume relations: a broader view. Circulation 1988;77:1203-12.
13. Freeman GL, Colston JT. Evaluation of long-term variance of left ventricular performance indexes in closed-chest dogs. Am J Physiol 1989;257:H70-8.
14. Kono A, Maughan WL, Sunagawa K, Hamilton K, Sugawa K, Weisfeldt ML. The use of left ventricular end-ejection pressure and peak pressure in the estimation of the end-systolic pressure-volume relationship. Circulation 1984;70:1057-65.
15. Alyono D, Larson VE, Anderson RW. Defining end-systole for end-systolic pressure-volume ratio. J Surg Res 1985;39: 344-50.
16. Rayhill SC, Castro LJ, Niczyporuk MA, et al. Rigid ring fixation of the mitral annulus does not impair left ventricular systolic function in the normal canine heart. Circulation 1992;86(Suppl):II26-38.
17. Castro LJ, Moon MR, Rayhill SC, et al. Annuloplasty with flexible or rigid ring does not alter left ventricular systolic performance, energetics, or ventricular-arterial coupling in conscious, closed-chest dogs. J THORAC CARDIOVASC SURG 1993;105:643-59.
18. Komoda T, Hetzer R, Uyama C, et al. Mitral annular function assessed by 3D imaging for mitral valve surgery. J Heart Valve Dis 1994;3:483-90.
19. van Rijk-Zwikker GL, Delemarre BJ, Huysmans HA. Mitral valve anatomy and morphology: relevance to mitral valve replacement and valve reconstruction. J Card Surg 1994; 9(Suppl):255-61.
20. Walmsley R. Anatomy of human mitral valve in adult cadaver and comparative anatomy of the valve. Br Heart J 1978;40: 351-66.
21. Brewer RJ, Deck JD, Capati B, Nolan SP. The dynamic aortic root: its role in aortic valve function. J THORAC CARDIOVASC SURG 1976;72:413-7.
22. Thubrikar M, Nolan SP, Bosher LP, Deck JD. The cyclic changes and structure of the base of the aortic valve. Am Heart J 1980;99:217-24.
23. Streeter DD. Gross morphology and fiber geometry of the heart. In: Bern RM, Sperelakis N, Geiger SR, eds. Handbook of physiology, section 2, The cardiovascular system, vol 1, The heart. Bethesda: American Physiological Society, 1979: 61-5.
24. Greenbaum RA, Ho SY, Gibson DG, Becker AE, Anderson

RH. Left ventricular fibre architecture in man. Br Heart J 1961;45:248-63.
25. Fernandez-Teran MA, Hurle JM. Myocardial fiber architecture of the human heart ventricles. Anat Rec 1982;204:137-47.
26. van Rijk-Zwikker GL, Schipperheyn JJ, Huysmans HA, Bruschke AVG. Influence of mitral valve prosthesis or rigid mitral ring on left ventricular pump function: a study on exposed and isolated blood-perfused porcine hearts. Circulation 1989;80(Suppl):I1-7.
27. van Rijk-Zwikker GL, Mast F, Schipperheyn JJ, Huysmans HA, Bruschke AVG. Comparison of rigid and flexible rings for annuloplasty of the porcine mitral valve. Circulation 1990;82(Suppl):IV58-64.
28. Kronzon I, Cohen ML, Winer HE, Colvin SB. Left ventricular outflow obstruction: a complication of mitral valvuloplasty. J Am Coll Cardiol 1984;4:825-8.
29. David TE, Komeda M, Pollick C, Burns RJ. Mitral valve annuloplasty: the effect of the type on left ventricular function. Ann Thorac Surg 1989;47:524-8.

## Discussion

**Dr. Richard Cochran** *(Seattle, Wash.).* I would like to express my encouragement to Dr. Glasson, who is joining in the quest for one of the Holy Grails of cardiac physiology—understanding the mitral anulus, its contraction, and its role in cardiac function.

The mitral valve, particularly the mitral anulus, has evaded evaluation and understanding because of its position, its anatomy, and the limitations in our technology. Dr. Glasson and her colleagues have developed an extensive and complex 17-marker system that allows for 3-D referencing of the mitral anulus and LV. They have developed and analyzed this sophisticated model with new computer software that is quite remarkable. It is this type of effort that we hope will eventually give us insight into the elusive problems and the role of the mitral anulus.

However, as a naive and somewhat "noncognitive" clinician, unsophisticated in some of these technologies, I am perplexed by these radical ideas. This paper seems to unsettle me more than enlighten me. I would like to ask several questions, first about the model.

You have chosen dogs as your experimental model. I know you have used this historically in your laboratory. In our laboratory and in others we have found that pigs more closely resemble the human anatomy and particularly the hematology. Can you tell us why you chose dogs?

**Dr. Glasson.** This experiment was the first to be performed in our laboratory directed at studying mitral anular motion in 3-D space. Current studies are now ongoing with sheep as the animal model, and we will have further data soon to follow. We do not believe the pig is more suitable (or more closely analogous to human beings), because pigs have small, very hypertrophied left ventricles.

**Dr. Cochran.** We do not think that the sheep is quite as accurate in its coronary anatomy as is the pig, but I think better and closer results can be obtained with a sheep model than a dog model.

You alluded also to the possibility of β-adrenergic blockade—and the concomitant decrease in LV function—as possibly having a role in this unusual finding. Did you repeat this study or have you plans to repeat this study in other animals that do not have β-adrenergic blockade to use them as a control for this variable.

**Dr. Glasson.** We do have an unblocked control group in the current ongoing studies with the sheep model. With dogs it is difficult to obtain satisfactory data without β-adrenergic blockade because of their very high heart rates; the dogs are mildly sedated, not anesthetized, during data acquisition and, therefore, have reflex sympathetic responses. It is quite difficult to visualize and track marker motion at a heart rate of 170 beats/min, making β-adrenergic blockade a useful tool for us in this respect. This is a limitation of the study, however, because LV contractility was depressed. We speculate such may affect mitral annular motion as well.

**Dr. Cochran.** I am confused about the markers. You describe them as nearly equidistant, but then you reference that markers 1 and 5 are at the commissures. Since that would leave three markers anteriorly and three markers posteriorly and the anterior anulus only makes up 33% to 40% of the circumferential area for the mitral valve in all species, what does this do to the distance between markers? Have you used any pathologic reference or anatomic references, such as putting them right at the commissures as a preferential way to do this?

**Dr. Glasson.** We chose the current marker placement system to generate eight segments of roughly similar lengths around the circumference of the mitral anulus. If we had used the trigones and commissures as anatomic reference points in this first study of mitral annular motion, then the segment between the left fibrous trigone and the anterolateral commissure, for example, would have been very short; therefore, changes in length of that segment might be difficult to detect. The first marker was placed at the middle of the anterior anulus; subsequently the second marker was placed at 90 degrees from the first, the third at 180 degrees, and the fourth at 270 degrees, resulting in four equal quadrants around the mitral anulus. The remaining four markers were placed to equally divide these quadrants into eight segments of similar lengths. It so happens that markers 1 and 5 lie in the proximity of the commissures, but they were not placed exactly at the commissures.

**Dr. Cochran.** But you have no pathologic markers for confirmation as far as references to the trigone?

**Dr. Glasson.** Markers 6 and 8 are in close proximity to the trigones, but they were not placed exactly on the trigones. Referring to the mitral annular marker schematic, marker 7 was the first to be placed, marker 5 was second, marker 3 was third, and marker 1 was fourth. Again, the markers were placed to divide the anulus into eight equal segments. After noting the segments of interest, as we did in this initial study of mitral annular motion, we are now able to focus future studies on defined anatomic landmarks, such as the fibrous trigones.

**Dr. Cochran.** My final question concerns your results and conclusions. As you mentioned, Tsakiris described in a similar study that half to two thirds of annular contraction occurs during atrial contraction and that during initial isovolumic ventricular contraction there was the suggestion of an increasing annular length. This seems to be confirmed by your data, in that before isovolumic contraction both segments 5 and 6 have an obvious shortening.

For segment 5 I am a bit concerned that this represents an increase in length that is just a return to baseline. This would be consistent with what Tsakiris has shown previously. Segment 6, however, does stick with your conclusions, that is, that there is an increase in length for that region, and I am a bit perplexed by that. As such, it leads to the questions I asked previously: As Tsakiris further points out in the same paper, the dog has collagenous tissue only at the trigone, so there is no true endoskeleton in the dog. I am concerned that this observation represents an increase in musculature in the dog anulus. If so, your conclusions may be a species anomaly that is specific to the dog and cannot be extrapolated to the human being.

**Dr. Glasson.** We analyzed the data extensively to decide which videofluoroscopic frames should be chosen to define the time of LV ejection using different definitions of end-diastole and end-systole, depending on the number of frames we moved forward or backward from the ECG R wave or from LV $-dP/dt_{max}$. When we did this, the statistical significance of changes in the length of segment 5 became marginal, and it may be true that this segment is not as important for normal mitral annular motion as is segment 6. No matter how we defined the time of LV ejection, however, we observed significant lengthening in segment 6. Indeed, it has been interesting to observe that sheep have much more muscle tissue in the mitral leaflets than do dogs, corresponding to your inference.

**Dr. Cochran.** My concern is that this area is just muscle and not an endoskeleton, as you would have in the human being, and as such these observations do not apply to the human being.

**Dr. Gerda van Rijk-Zwikker** *(Leiden, The Netherlands).* I have some questions regarding the correlation between anatomy and function of the mitral valve with respect to the anterior leaflet. What concerns me is that I think you are overlapping muscle and fibrous tissue and that you see lengthening of muscle and fibrous tissue. Furthermore, the hinge line of the anterior leaflet is at the bottom of the trigone of the aortomitral membrane, whereas your markers are at the anatomic border, which is actually the aortic outflow tract. I think you are measuring the expansion of the outflow tract rather than functional widening of the mitral valve anulus.

**Dr. Glasson.** That is an excellent point, as evidenced by previous work on the dynamic aortic root performed by Dr. Stanton Nolan's group at the University of Virginia. When I first analyzed these data, I also thought that the lengthening we observed in the anterior anulus could be explained by aortic root expansion. What is different, however, is that Dr. Nolan's data indicate that aortic root expansion occurs primarily during early systole, and our data show anterior annular lengthening, especially in segment 6, throughout the entire period of LV ejection. Additionally, peak lengthening occurred during late systole. Regarding the actual structure we studied, if the tissue in the area of lengthening were in fact muscle, then I would expect it to contract and shorten during LV ejection, not lengthen, as we observed.

**Dr. van Rijk-Zwikker.** We have shown that expansion of the aortic inflow through the ventriculoarterial junction is actually throughout systole.

**Dr. Glasson.** This is another excellent point. Future studies in our laboratory may be performed with markers placed on specific anatomic landmarks to define more precisely exactly what portions of the mitral anulus are lengthening or shortening.